DOI: 10.1002/chem.201000028

Thermal Decomposition of Mono- and Bimetallic Magnesium Amidoborane Complexes

Jan Spielmann, Dirk F.-J. Piesik, and Sjoerd Harder*[a]

Abstract: Complexes of the type [(DIPPnacnac)MgNH(R)BH_3] have been prepared (DIPPnacnac = CH-{(CMe)(2,6-*i*$Pr_2C_6H_3N$)}$_2$). The following substituents R have been used: H, Me, *i*Pr, DIPP (DIPP = 2,6-diisopropylphenyl). Complexes [(DIPPnacnac)MgNH_2BH_3]·THF, [{(DIPPnacnac)MgNH(*i*Pr)BH_3}$_2$] and [(DIPPnacnac)MgNH(DIPP)BH_3] were structurally characterised. The Mg amidoborane complexes decompose at a significantly higher temperature (90–110 °C) than the corresponding Ca amidoborane complexes (20–110 °C). The complexes with the smaller R substituents (H, Me) gave a mixture of decomposition products of which one could be structurally characterised as [{(DIPPnacnac)Mg}$_2$(H_3B-NMe-BH-NMe)]·THF. [{(DIPPnacnac)MgNH(*i*Pr)BH_3}$_2$] cleanly decomposed to [(DIPPnacnac)MgH], which was characterised as a dimeric THF adduct. The amidoborane complex with the larger DIPP-substituent decomposed into a borylamide complex [(DIPPnacnac)MgN(DIPP)BH_2], which was structurally characterised as its THF adduct. Bimetallic Mg amidoborane complexes decompose at lower temperatures (60–90 °C) and show a different decomposition pathway. The dinuclear Mg amidoborane complexes presented here are based on DIPPnacnac units that are either directly coupled through N–N bonding (abbreviated **NN**) or through a 2,6-pyridylene bridge (abbreviated **PYR**). Crystal structures of [**PYR**-{Mg(*n*Bu)}$_2$], [**PYR**-{MgNH(*i*Pr)BH_3}$_2$], [**NN**-{MgNH(*i*Pr)BH_3}$_2$]·THF and the decomposition products [**PYR**-Mg_2(*i*PrN-BH-*i*PrN-BH_3)] and [**NN**-Mg_2(*i*PrN-BH-*i*PrN-BH_3)]·THF are presented. The following conclusions can be drawn from these studies: i) The first step in the decomposition of a metal amidoborane complex is β-hydride elimination, which results in formation of a metal hydride complex and R(H)N=BH_2, ii) depending on the nature of the metal, the metal hydride is either stable and can be isolated or it reacts further, iii) amidoborane anions with small R substituents decompose into the dianionic species (RN-BH-RN-BH_3)$^{2-}$, whereas large substituents result in formation of the borylamide RN=BH_2^- and iv) enforced proximity of two Mg amidoborane units results in decomposition at a significantly lower temperature and cleanly follows the BNBN pathway.

Keywords: alkaline earth metals · boranes · bimetallic complexes · hydrogen storage · magnesium

Introduction

The early main group metal amidoboranes $LiNH_2BH_3$, $NaNH_2BH_3$ and $Ca(NH_2BH_3)_2$ have been recently introduced as very promising hydrogen-storage materials that fulfil the current DOE requirements for on-board storage systems.[1,2] These compounds not only eliminate hydrogen at a much lower temperature than the parent ammonia–borane (NH_3BH_3),[3] but also show less foaming and no undesirable by-products such as borazine. As hydrogen release for these metal species is nearly thermoneutral, they are excellent candidates for investigations concerning reversibility. This would allow for recycling by simple hydrogenation with molecular hydrogen, thus circumventing multi-step chemical routes.[4] Any research activity in this area would greatly benefit from a detailed understanding of the dehydrogenation process and the products formed.

We recently introduced the concept of converting these solid-state materials into soluble molecular model systems.[5,6] Reactions of ammonia–borane (or *N*-substituted ammonia–boranes) with organometallic precursors gave a

[a] J. Spielmann, D. F.-J. Piesik, Prof. Dr. S. Harder
Anorganische Chemie
Universität Duisburg–Essen
Universitätsstrasse 5, 45117 Essen (Germany)
Fax: (+49) 201-1832621
E-mail: sjoerd.harder@uni-due.de

Supporting information for this article contains the details of the crystal structure determinations and crystal data and is available on the WWW under http://dx.doi.org/10.1002/chem.201000211.

variety of heteroleptic metal amidoborane complexes that contain the bulky bidentate β-diketiminate ligand DIPPnacnac, $CH\{(CMe)(2,6\text{-}iPr_2C_6H_3N)\}_2$ (Scheme 1). This ligand

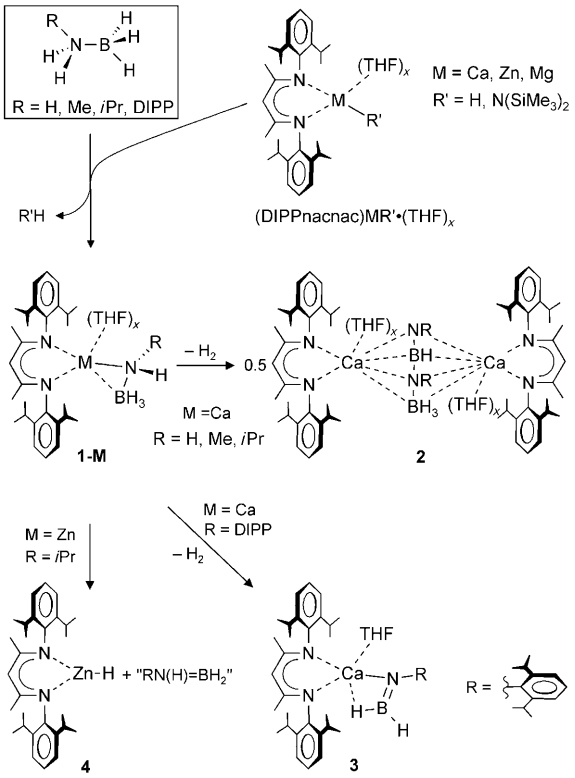

Scheme 1. Overview of the formation and decomposition of metal amidoborane complexes.

solubilises the amidoborane functionality and prevents ligand-exchange reactions that might generate insoluble homoleptic metal-amidoborane complexes like $[M(NH_2BH_3)_2]$ (M = Mg, Ca, Zn). This approach not only allows for a detailed study of the metal amidoborane complexes themselves, but also facilitates investigations concerning the dehydrogenation of these species. Thus, we have been able to elucidate the decomposition product for the dehydrogenation of the soluble calcium amidoborane complex $[(DIPPnacnac)CaNH_2BH_3]\cdot(THF)_2$ (**1-Ca**, R = H), which can eliminate H_2 at the record low temperature of 20 °C.[5] The decomposition product (**2**, R = H) is a soluble molecular species that was crystallised and structurally characterised as a dimeric complex that contains the novel bridging dianionic species $(HN\text{-}BN\text{-}NH\text{-}BH_3)^{2-}$. All attempts to reverse this reaction by pressurising a solution of this product with H_2 under various conditions failed. As the energetically favourable newly formed B–N bond might be the origin of this non-reversible reaction behaviour, we introduced substituents on N that prevent this dimerisation reaction. Whereas Me and *i*Pr substituents still allow for formation of BNBN species (**2**, R = Me or *i*Pr), the larger 2,6-diisopropylphenyl (DIPP) substituent could prevent B–N bond formation and crystals of the borylamide complex $[(DIPPnacnac)CaN(DIPP)BH_2]\cdot THF$ (**3**) were isolated in 71% yield.[6] Likewise, also **3** could not be hydrogenated by pressurising a solution with H_2 under various reaction conditions.

As part of a systematic study on the effect of the metal in these reactions, we preliminarily reported on the attempted synthesis of zinc amidoborane complexes (**1-Zn**).[7] Hitherto, such complexes could not be isolated and in one case monomeric [(DIPPnacnac)ZnH] (**4**) was obtained in 71% crystalline yield. This shows that ammonia-borane reagents are also useful precursors in the syntheses of metal-hydride complexes.

Our preliminary investigations on magnesium amidoborane complexes showed that attempted conversion of the $[(DIPPnacnac)MgN(SiMe_3)_2]$ with $(DIPP)NH_2BH_3$ led to catalytic decomposition of the ammonia-borane into $HB[N(DIPP)H]_2$, BH_3 and H_2.[8] It was proposed that intermediate [(DIPPnacnac)MgH] could play an important role in the catalytic cycle.

The examples above illustrate that metal effects are crucial for the stability and decomposition pathways of metal amidoborane complexes. Our earlier, simplified, chart of possible decomposition pathways for **1-Ca** (R = H) did not incorporate the metals.[6] Here we report on the synthesis of a series of magnesium amidoborane complexes, comment on their thermal decomposition pathways, discuss differences with analogous calcium species and propose possible mechanistic routes that include the role of the metal. The proposed mechanisms are in line with recent theoretical studies on the decomposition of $LiNH_2BH_3$.[9,10] To strengthen our views on the mechanism, we also present binuclear magnesium amidoborane complexes, which behave differently from mononuclear species. These bimetallic amidoborane complexes are more realistic model systems for a solid-state situation in which more than one metal nucleus could be involved in the decompostion pathway.

Results and Discussion

Monometallic magnesium amidoborane complexes: Heteroleptic magnesium amidoborane complexes with the supporting DIPPnacnac ligand and a variety of substituents on the amidoborane nitrogen atom (**1-Mg**, R = H, Me, *i*Pr) could be obtained by addition of the corresponding ammonia-borane precursor to a benzene solution of $[(DIPPnacnac)MgN(SiMe_3)_2]$ (Scheme 2). In all cases the products conveniently separated from solution in the form of crystals. This synthetic approach was not successful for the synthesis of the amidoborane complex with the large DIPP substituent. In this particular case, the starting reagent $[(DIPPnacnac)MgN(SiMe_3)_2]$ acts as a catalyst for the decomposition of $DIPPNH_2BH_3$ into $HB[NH(DIPP)]_2$, BH_3 and H_2.[8] However, as we reported earlier, the Mg amidoborane complex is accessible by using the more reactive $[\{(DIPPnacnac)MgH\}_2]$, a reagent recently introduced by Jones et al. (Scheme 2).[11]

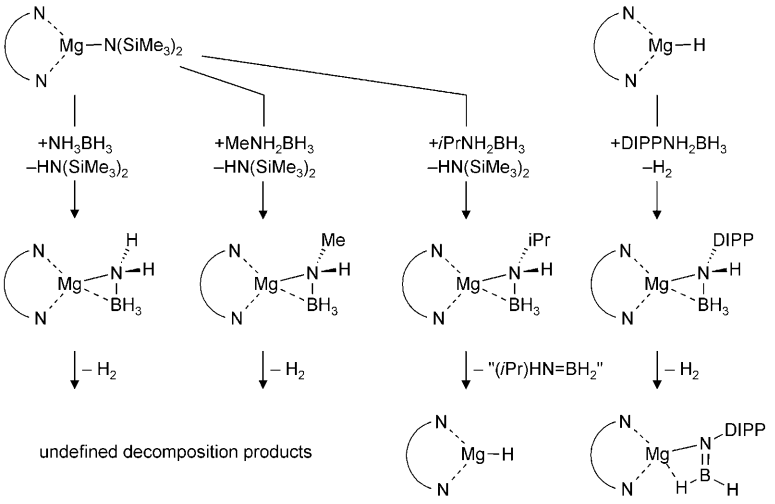

Scheme 2. Syntheses and decomposition of magnesium amidoborane complexes (in all cases the bidentate chelating ligand is the DIPPnacnac ligand).

Structural characterisation by single crystal X-ray diffraction was in some cases hindered by unsolvable disorder of the amidoborane anions. These anions were also found to be notorious for unordered behaviour in earlier studies.[5] The complex [(DIPPnacnac)$MgNH_2BH_3$] crystallised from benzene/THF, as a THF-free dimer with bridging NH_2BH_3 anions for which the exact positions could not be defined. Crystallisation of this complex from a hexane/THF solution, however, gave crystals of the monomeric THF adduct [(DIPPnacnac)$MgNH_2BH_3$]·(THF). This complex was unambiguously characterised by a crystal structure determination and shows a side-on coordinated $NH_2BH_3^-$ ion (Figure 1 a). The complex with a Me substituent on N crystallised from benzene/THF, as the THF adduct [(DIPPnacnac)MgNH(Me)BH_3]·THF, but could not be structurally characterised on account of poor crystal quality. The amidoborane complex [(DIPPnacnac)MgNH(*i*Pr)BH_3] crystallised from benzene, as a well-ordered centrosymmetric dimer with amidoborane units that bridge the two Mg^{2+} ions (Figure 1 b). [(DIPPnacnac)MgNH(DIPP)BH_3] crystallised from toluene as a THF-free monomer with a side-on coordinated amidoborane unit. A detailed description of its crystal structure can be found in a preliminary communication.[8] The considerable steric bulk of the DIPP substituent apparently prevents dimerisation.

Selected bond lengths for all crystal structures are summarised in Table 1. The metals in the previously published calcium amidoborane complexes[5,6] show coordination numbers and geometries that are different from those in the magnesium amidoborane complexes. Although this makes a comparison of the geometrical parameters in these two sets of complexes difficult, in general the same trends can be observed. Increasing the steric bulk on the amidoborane N atom results in lengthening of the metal–N bond with concomitant shortening of the metal···B contact. The ratio metal-N/metal···B in [(DIPPnacnac)$CaNH_2BH_3$]·$(THF)_2$ and [(DIPPnacnac)$MgNH_2BH_3$]·THF is nearly similar (0.836 and 0.841, respectively). For the bulkier complexes [(DIPPnacnac)CaNH(DIPP)-BH_3]·THF and [(DIPPnacnac)MgNH(DIPP)BH_3] larger ratios of 0.957 and 0.909, respectively, are found.

Interestingly the B–N bond lengths for calcium amidoborane complexes are not influenced by the various substituents (range 1.581(4)–1.587(4) Å, average 1.583(4) Å).[6] The B–N bonds in the magnesium amidoborane complexes, however, are in a much broader range of 1.544(6)–1.626(8) Å (average 1.575(8) Å). They seem to increase with increasing bulk of the substituent on N and reach a maximum of 1.626(8) Å for [(DIPPnacnac)MgNH(DIPP)BH_3].

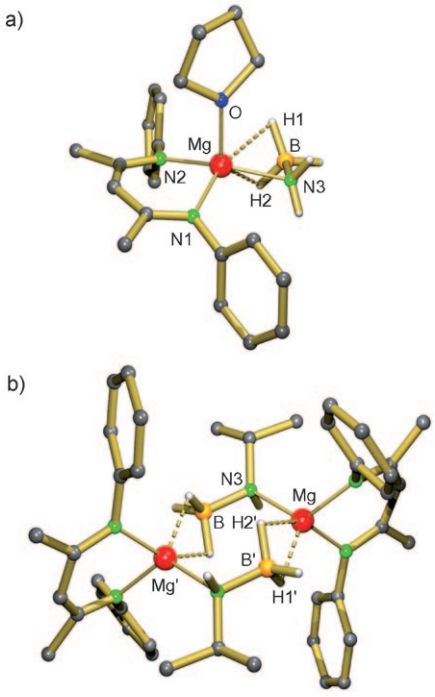

Figure 1. The crystal structures of a) [(DIPPnacnac)$MgNH_2BH_3$]·THF and b) [{(DIPPnacnac)MgN(*i*Pr)HBH_3}$_2$]. For clarity, the *i*Pr substituents on the DIPPnacnac ligands have been omitted and only the hydrogen atoms on B and N are shown. Selected bond lengths are summarised in Table 1.

Except for the amidoborane complex with the DIPP substituent, all products are poorly soluble in aromatic solvents. Addition of small amounts of THF, however, solubilises these compounds and it is likely that aggregates break down to monomers on account of THF–Mg interaction (Figure 1 a). The complexes were fully characterised by ^1H, ^{13}C

Table 1. Selected bond lengths for mononuclear Mg complexes and their decomposition products (Å).

[(DIPPnacnac)MgNH$_2$BH$_3$]·THF					
Mg–N1	2.071(3)	Mg–O	2.055(2)	Mg···H2	2.48
Mg–N2	2.071(3)	Mg···B	2.463(5)	B–N	1.544(6)
Mg–N3	2.056(3)	Mg···H1	2.47		
[{(DIPPnacnac)MgNH(*i*Pr)BH$_3$}$_2$]					
Mg–N1	2.056(1)	Mg–B′	2.417(2)	B–N3	1.556(2)
Mg–N2	2.074(1)	Mg···H1	1.94(2)	Mg···Mg′	4.1413(6)
Mg–N3	2.122(1)	Mg···H2	2.01(2)		
[{(DIPPnacnac)Mg}$_2$(H$_3$B-NMe-BH-NMe)]·THF					
Mg1–N1	2.075(1)	Mg1–H1	2.42(2)	Mg2–H2	2.22(2)
Mg1–N2	2.072(1)	Mg2–N3	2.039(1)	Mg2–H3	1.97(2)
Mg1–N6	2.099(1)	Mg2–N4	2.079(1)	N5–B1	1.371(3)
Mg1–O	2.049(1)	Mg2–N5	2.016(1)	B1–N6	1.491(3)
Mg1···B2	2.607(2)	Mg2···B2	2.433(2)	N6–B2	1.556(3)
[(DIPPnacnac)MgN(DIPP)BH$_2$]·THF					
Mg–N1	2.066(2)	Mg–O1	2.063(2)	B–N	1.371(3)
Mg–N1′	2.066(2)	Mg···B	2.624(3)		
Mg–N2	2.026(2)	Mg···H1	2.38(3)		

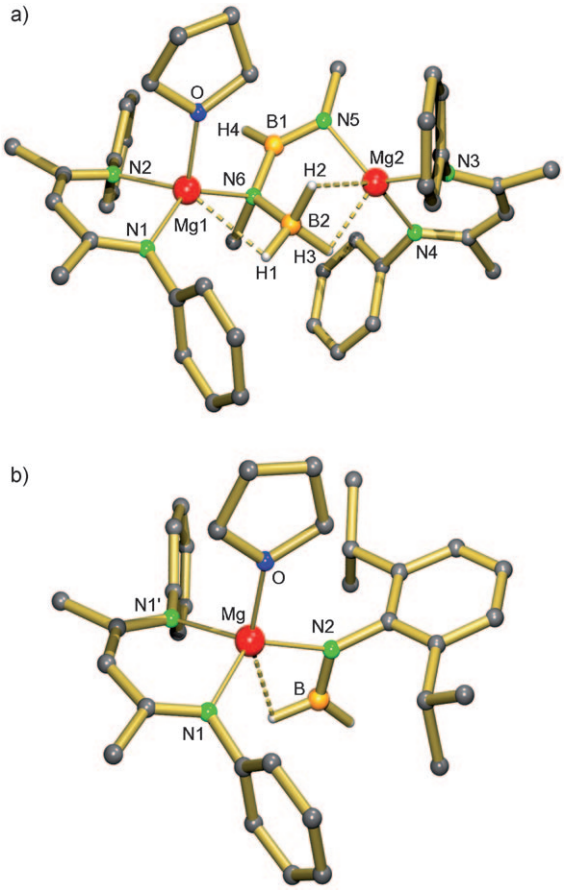

Figure 2. Crystal structures of a) [{(DIPPnacnac)Mg}$_2$(H$_3$B-NMe-BH-NMe)]·THF and b) [(DIPPnacnac)MgN(DIPP)BH$_2$]·THF. For clarity, the *i*Pr substituents on the DIPPnacnac ligands have been omitted and only the hydrogen atoms on B are shown. Selected bond lengths are summarised in Table 1.

and ^{11}B NMR spectroscopy in benzene/THF mixtures. The ^{1}H NMR signals for NH appear between $\delta = -0.40$ and -0.51 ppm, except for [(DIPPnacnac)MgNH(DIPP)BH$_3$] in which its aniline-like character causes a low-field shift to $\delta =$ 2.86 ppm. The ^{1}H NMR signals for BH$_3$ can be found in the range $\delta = 1.63$–2.44 ppm (^{11}B NMR range: $\delta = -17.7$/ -22.4 ppm).

In the next stage of our studies, the thermal decomposition of the four magnesium amidoborane complexes in Scheme 2 was evaluated. In general, the decomposition temperatures were found to be substantially higher than those for the analogous calcium amidoborane complexes. Whereas the calcium complexes with small substituents on the amidoborane anion ($NH_2BH_3^-$ or $MeNHBH_3^-$) release H_2 already in the temperature range of 20–40 °C, analogous magnesium complexes need much more forcing reaction conditions of temperatures of >80 °C. Thermal decomposition of [(DIPPnacnac)MgNH$_2$BH$_3$] and [(DIPPnacnac)MgN(Me)HBH$_3$] dissolved in benzene was not clean and several unidentified species could be observed in the ^{1}H NMR spectra. Repeated attempts to isolate well-defined products from these mixtures failed, however, thermal decomposition of [(DIPPnacnac)MgNH(Me)BH$_3$]·THF gave a few crystals of one of the decomposition products. Crystal structure analysis revealed the complex [{(DIPPnacnac)Mg}$_2$(H$_3$B-NMe-BH-NMe)]·THF (Figure 2a). The dianionic species (H$_3$B-NMe-BH-NMe)$^{2-}$ shows a long-short-short B-N-B–N bond pattern as in the analogue Ca complex.[5] In contrast, however, this dianionic species bridges asymmetrically between the metal centres.

[(DIPPnacnac)MgNH(*i*Pr)BH$_3$] in benzene decomposed at the even higher temperature of 110 °C (in this case a sealed tube was used). After prolonged heating of the sample (16 h) the ^{1}H NMR spectrum showed signals for two single decomposition products and H_2 could be observed ($\delta = 4.47$ ppm). Addition of hexane resulted in precipitation of a white powder for which ^{1}H and ^{13}C NMR data correspond to those for the earlier reported [{(DIPPnacnac)MgH}$_2$].[11] From ^{1}H, ^{13}C and ^{11}B NMR data we conclude that the amidoborane part cleanly reacted to the borazine (*i*PrNBH)$_3$ (see the Experimental Section). This is likely formed by condensation of three molecules of *i*PrNH=BH$_2$ followed by H_2 elimination. The latter process is likely catalysed by the magnesium hydride base.

The 89% yield of [{(DIPPnacnac)MgH}$_2$] and the relatively short reaction time of 16 h makes this decomposition route an attractive preparative procedure (see the reaction of [(DIPPnacnac)MgBu] with PhSiH$_3$ gave after 2 days the product in 40% yield).[11] Recrystallisation of the product from a toluene/hexane/THF mixture gave crystals of the THF adduct, which could be structurally characterised as the dimer [{(DIPPnacnac)MgH·(THF)}$_2$]. Although it crystallises in a different unit cell from that reported earlier,[11] this new polymorph displays very similar characteristics—both are centrosymmetric dimers with coplanar DIPPnacnac units and the bridging hydride ions roughly reside in the same plane. Also bond lengths and angles are very much

comparable (details can be found in the Supporting Information). Interestingly, the crystals obtained here are isomorphic to [{(DIPPnacnac)YbH·(THF)}$_2$][12] a complex with much larger metal cations (Yb^{2+} 1.02 Å, Mg^{2+} 0.72 Å).[13]

The complex with the most bulky amidoborane ligand, [(DIPPnacnac)MgNH(DIPP)BH_3], only decomposed under forcing conditions. Like the analogous calcium complex [(DIPPnacnac)CaNH(DIPP)BH_3]·THF, a benzene solution of the magnesium complex was kept for 24 h at 120 °C. The ^{1}H NMR spectrum showed clean decomposition into one species and a clear singlet at $\delta = 4.47$ ppm was conclusive for substantial H_2 production. Crystallisation of the isolated product from a hexane/toluene/THF mixture gave the borylamide complex [(DIPPnacnac)MgN(DIPP)BH_2]·THF. This complex was characterised by using ^{1}H, ^{13}C and ^{11}B NMR spectroscopy, as well as X-ray diffraction. Similar to **3** it crystallises as a mirror-symmetric, monomeric species with a side-on coordinated borylamide ligand and one THF ligand in the coordination sphere (Figure 2b). The B–N bond, which dependent on the extent of $2p_N$–$2p_B$ overlap could be seen as having double bond character (B=N), is with 1.371(3) Å considerably shorter than that in the amidoborane precursor (1.626(8) Å). It is, however, somewhat longer than the comparable B–N bond in the calcium borylamide complex **3** (1.353(3) Å). This is likely owed to the more covalent bonding in the magnesium complex: a less negatively charged borylamide ion DIPPN=$BH_2^{\delta-}$ should also display less extensive $2p_N \rightarrow 2p_B$ donation. Although this might facilitate the reversible hydrogenation of this B=N bond, all attempts to hydrogenate [(DIPPnacnac)MgN(DIPP)BH_2] with H_2 (1–100 bar) failed.

Comparison with earlier work on similar Ca[5] and Zn[7] amidoborane complexes shows that the course of thermal decomposition can be strongly metal dependant. Different decomposition temperatures and decomposition products are observed. We proposed earlier that the Ca complex [(DIPPnacnac)CaNH_2BH_3]·$(THF)_2$ likely eliminates H_2 via a binuclear dimeric intermediate (Scheme 3). This proposal is based on the observation that a THF solution of this complex is thermally stable and only eliminates H_2 at temperatures >100 °C, whereas in benzene smooth formation of H_2 already proceeds at 20 °C. It is, therefore, likely that the first step is loss of THF from the metal's coordination sphere. This could induce the formation of a dimeric intermediate, which would enable favourable contacts between hydridic and protic hydrogen atoms belonging to different amidoborane ions. These N–H$^{\delta+}$···H$^{\delta-}$–B bonds are considered weak ($\approx$4 kcal mol^{-1}),[14] but are also found in the crystal structure of NH_3BH_3 and are responsible for its solid existence at standard conditions.[15] Intramolecular elimination of H_2 within an amidoborane unit is a high energy process,[9,10] but N–H$^{\delta+}$···H$^{\delta-}$–B interactions between amidoborane units within a dimer might lower the transition state considerably. It was therefore expected that the dimeric complex [{(DIPPnacnac)MgNH(*i*Pr)BH_3}$_2$] would release H_2 at a relatively low temperature. However, in benzene the complex only slowly starts to decompose at 80 °C. Heating the compound overnight at 110 °C led to formation of a distinct decomposition product. There is no experimental information on the aggregation state of the amidoborane complex in benzene solution. Crystals of the dimer only dissolve at a temperature >60 °C and it is likely that under these conditions entropy effects break the dimer into soluble monomeric units. This could explain the rather high decomposition temperature. The decomposition reaction is clean and only [{(DIPPnacnac)MgH}$_2$] and (*i*PrNBH)$_3$ can be observed. In contrast, the similar Ca amidoborane complex decomposed to a product containing the BNBN species (*i*PrN-BH-N*i*Pr-BH_3)$^{2-}$ (Scheme 1).

These differences between Mg and Ca chemistry can be discussed in the light of recent theoretical work by Kim et al. on the thermal decomposition of $LiNH_2BH_3$.[9] Although the authors were seemingly unaware of the experimental work on analogous calcium amidoborane complexes, it is interesting to note that these theoretical considerations conclude two important aspects: i) Decomposition of dimeric metal amidoborane complexes is favoured over that in monomeric model systems and ii) the main low-energy pathway diverges to decomposition products known from experimental work, that is, the [HN-BH-NH-BH_3]$^{2-}$ ion or the borylamide ion HN=BH_2^-.[5,6]

Kim et al. calculated that direct (intramolecular) H_2 elimination in monomeric $LiNH_2BH_3$ needs the high activation energy of 59 kcal mol^{-1} (Scheme 4). Even scission of the B–N bond, to give $LiNH_2$ and BH_3, would be lower in energy (55 kcal mol^{-1}). Formation of the borylamide product $LiNHBH_2$ via a β-hydride elimination pathway is clearly favoured (33 kcal mol^{-1}).[9] Dimerisation of two $LiNH_2BH_3$ species is calculated to be exothermic by 36 kcal mol^{-1}. β-Hydride elimination in a dimeric aggregate is even more favourable: an activation energy of 27 kcal mol^{-1} has been calculated (Scheme 5). The product consists of a mixed hydride/amidoborane dimer with a coordinated neutral H_2B=NH_2 fragment. At this point the pathway splits: H_2B=NH_2 is either attacked by the amidoborane nucleophile, thus resulting in formation of a BNBN species, or it is deprotonated by the hydride base, in which case a borylamide is formed. The overall activation energy for the borylamide pathway (47 kcal mol^{-1}) is considerably higher than that for the

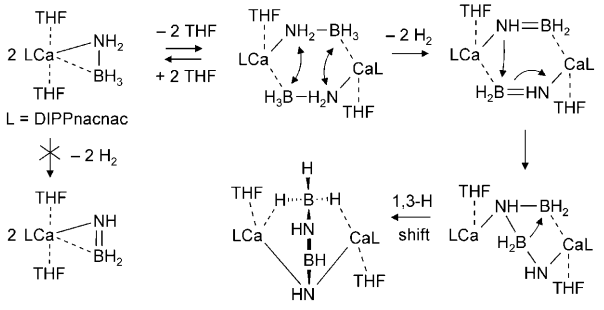

Scheme 3. The elimination of H_2 from [(DIPPnacnac)CaNH_2BH_3]·$(THF)_2$ has been proposed to proceed through a dimeric intermediate in which NH···HB protic–hydridic interactions could play an important role.

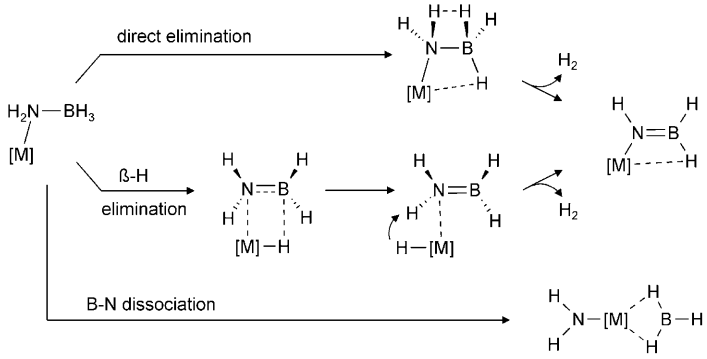

Scheme 4. General decomposition pathways for monomeric metal amidoborane complexes. For $LiNH_2BH_3$ the following activation energies have been calculated: direct elimination of H_2 = 59 kcal mol^{-1}, β-H elimination and subsequent borylamide formation = 33 kcal mol^{-1} and B–N dissociation = 55 kcal mol^{-1}.[9]

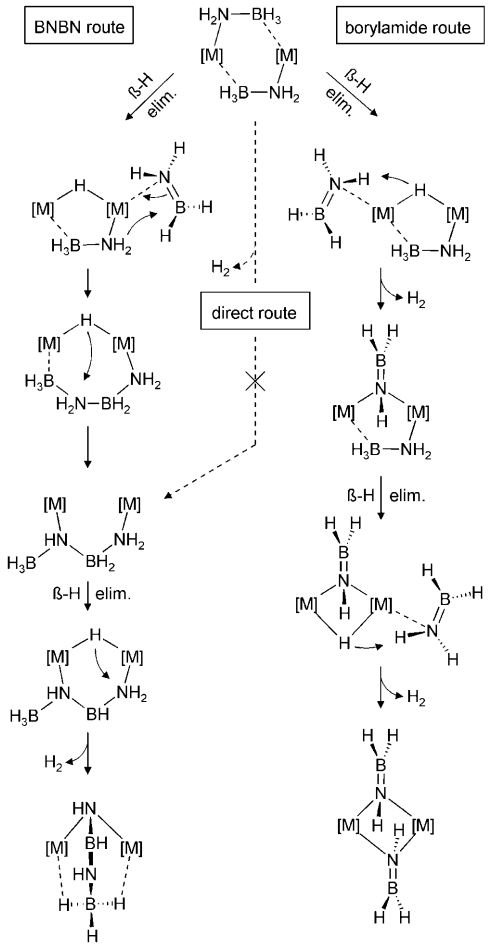

Scheme 5. General decomposition pathways for dimeric metal amidoborane complexes. For $(LiNH_2BH_3)_2$ the following activation energies have been calculated: BNBN route = 34 kcal mol^{-1} and the borylamide route = 47 kcal mol^{-1}.[9]

BNBN pathway (34 kcal mol^{-1}). Unfortunately, the direct H_2 elimination route was not evaluated for the dimeric model system. As proposed in Scheme 3, combination of hydridic and protic hydrogen atoms of different amidoborane units could be a low-energy pathway for H_2 elimination. Our attempts to optimise a reasonable theoretical model for such a transition state, however, failed and only led to high energy geometries.[16] Therefore, β-hydride elimination is the likely key step and metal hydride complexes are the first intermediates in all decomposition schemes.

The pathways sketched in Schemes 4 and 5 explain the experimentally observed decomposition products of Mg and Ca amidoborane complexes. Calcium amidoborane complexes with smaller substituents on N (H, Me, *i*Pr) were found to decompose at lower temperatures and generally follow the lowest energy pathway, the BNBN route. A very large DIPP-substituent on N prevents this decomposition route and forces it to follow the higher energy pathway, the borylamide route. This is in agreement with our experimentally observed high decomposition temperature of 110 °C.

It is likely that β-hydride elimination is also the first step in the decomposition of magnesium amidoborane complexes. However, the more covalently bound Mg intermediates are less reactive than the analogous Ca intermediates. The in situ generated $R(H)N{=}BH_2$ could therefore escape the metal's coordination sphere and oligomerise to $[R(H)NBH_2]_n$. Considering the high reaction temperatures needed for decomposition of Mg amidoborane complexes, loss of $R(H)N{=}BH_2$ would entropically also be favoured. Thus $[\{(DIPPnacnac)MgNH(iPr)BH_3\}_2]$ is nearly quantitatively converted into $[\{(DIPPnacnac)MgH\}_2]$ and $[iPr(H)NBH_2]_3$. The sterically protected $DIPP(H)N{=}BH_2$, however, less likely oligomerises and is also more acidic than $iPr(H)N{=}BH_2$. At the harsh reaction conditions (120 °C) it should be deprotonated by the intermediate hydride complex to give the borylamide complex $[(DIPPnacnac)MgN(DIPP)BH_2]$.

Whereas Ca amidoborane complexes show strong preference for the BNBN decomposition pathway, the analogous Mg complexes decompose to a variety of products and only in one case could we crystallise trace amounts of the BNBN product. Can this difference solely be ascribed to the higher reactivity of Ca complexes in general or do aggregation effects play a role? So far we have no information on the aggregation state of the metal amidoborane precursors in solution, however, Ca complexes have a higher tendency to aggregate than their congeners with smaller Mg cations. A dimeric state could facilitate the BNBN pathway considerably. In a monomeric model BNBN products can only be realised by intermolecular reaction of the in situ formed $R(H)N{=}BH_2$ and the precursor $LM[NH(R)BH_3]$. To shed light on the importance of nuclearity, we prepared two different dinuclear Mg amidoborane complexes and studied their decomposition behaviour.

Bimetallic magnesium amidoborane complexes: We recently introduced a set of dinucleating bis(β-diketiminate) ligands in which DIPPnacnac units are either connected directly by N–N bonding or through a rigid bridge (1,4-phenylene, 1,3-phenylene or 2,6-pyridylene).[17,18] In our studies described in here we focussed on two of these ligands, the 2,6-pyridy-

lene bridged ligand abbreviated in here as **PYR** and the directly N–N coupled ligand (no bridge at all) abbreviated here as **NN** (Scheme 6).

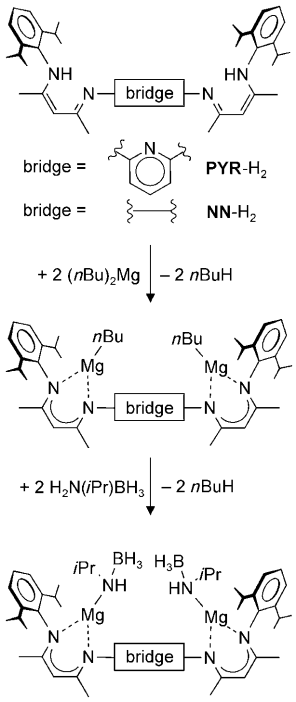

Scheme 6. Syntheses of dinuclear Mg amidoborane complexes with coupled DIPPnacnac ligands.

Reaction of the ligands **PYR**-H_2 and **NN**-H_2 with $(n\mathrm{Bu})_2\mathrm{Mg}$ in benzene/heptane at room temperature gave the binuclear complexes [**PYR**-{Mg(nBu)}$_2$] and [**NN**-{Mg(nBu)}$_2$], as THF-free crystalline products. The crystal structure of [**PYR**-{Mg(nBu)}$_2$] shows a C_2-symmetric complex in which the nBu anions bridge between the Mg^{2+} ions (Figure 3a, Table 2). The slight asymmetry in bridging (Mg–C1 2.233(3), Mg′–C1 2.312(3) Å) is caused by an agostic Mg···α-CH_2 interaction with only one of the hydrogen atoms (Mg···H 2.13(3) Å). Bridging nBu anions also create considerable strain in the pyridylene ring; the exocyclic C-C-N2 angle is widened to 130.9(3)° and N3-C-N2 is squeezed to 109.8(2)°. The coordination sphere of both Mg^{2+} ions is saturated by the bidentate nacnac units in which the terminal N atom (N1) is typically slightly more remote than the internal N atom (N2). Also the pyridyl bridge (N3), coordinates to both Mg^{2+} ions, however, this contact is much longer and should be considered weak. So far, no crystals of THF-free [**NN**-{Mg(nBu)}$_2$] have been obtained, however, we recently published the crystal structure of the THF adduct [**NN**-{CaN(SiMe$_3$)$_2$·THF}$_2$], which shows a binuclear complex with terminal, non-bridging, $(Me_3Si)_2N$ ligands.[18]

The binuclear Mg complexes [**PYR**-{Mg(nBu)}$_2$] and [**NN**-{Mg(nBu)}$_2$] dissolve well in benzene and react at room temperature smoothly with $i\mathrm{PrNH_2BH_3}$ to give the corresponding amidoborane complexes [**PYR**-{MgNH-

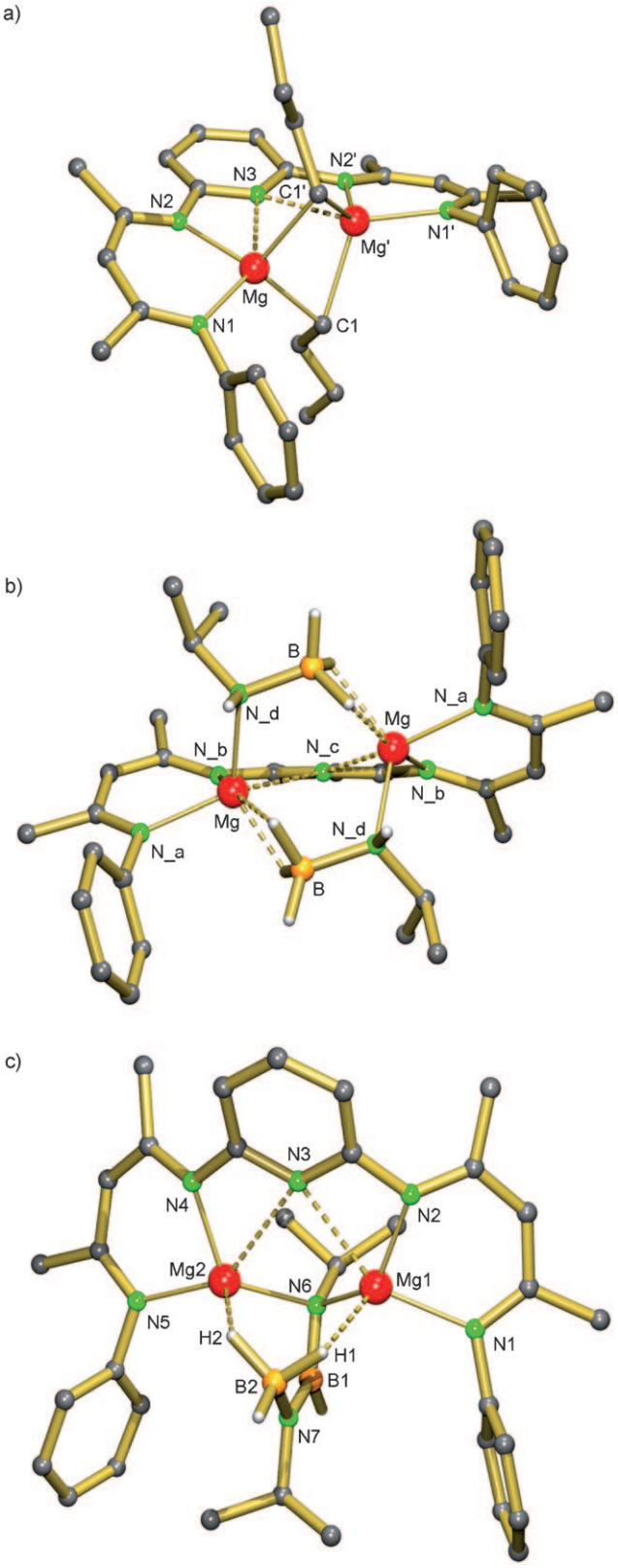

Figure 3. The crystal structures of a) [**PYR**-{Mg(nBu)}$_2$], b) [**PYR**-{MgNH(iPr)BH$_3$}$_2$] and c) [**PYR**-Mg$_2$(iPrN-BH-iPrN-BH$_3$)]. For clarity, the iPr substituents on the DIPPnacnac ligands have been omitted and only the hydrogen atoms on B are shown. Selected bond lengths are summarised in Table 2.

Table 2. Selected bond lengths for dinuclear Mg complexes (Å).

[**PYR**-{Mg(*n*Bu)}$_2$]					
Mg–N1	2.114(3)	Mg–N3	2.459(2)	Mg–C1	2.233(3)
Mg–N2	2.053(2)	Mg···Mg′	2.631(1)	Mg–C1′	2.312(3)
[**PYR**-{MgNH(*i*Pr)BH$_3$}$_2$] (range and average values given)					
Mg–N_a	2.085(4)–2.101(4) ⟨2.095(4)⟩	Mg–N_d	2.112(4)–2.134(3) ⟨2.123(4)⟩	Mg···Mg′	3.443(2)–3.473(2) ⟨3.458(2)⟩
Mg–N_b	2.016(4)–2.030(4) ⟨2.022(4)⟩	Mg···B	2.437(5)–2.464(5) ⟨2.449(5)⟩	B–N	1.555(6)–1.587(6) ⟨1.571(6)⟩
Mg–N_c	2.675(4)–2.712(3) ⟨2.692(4)⟩	Mg···H	1.92(3)–2.19(3) ⟨2.04(3)⟩		
[**PYR**-Mg$_2$(*i*PrN-BH-*i*PrN-BH$_3$)]					
Mg1–N1	2.129(1)	Mg1–N3	2.551(2)	Mg1···B2	2.775(2)
Mg1–N2	2.038(2)	Mg1–N6	2.056(1)	Mg1···H1	1.98(2)
Mg2–N4	2.050(2)	Mg2–N3	2.739(2)	Mg2···B2	2.689(2)
Mg2–N5	2.093(2)	Mg2–N6	2.079(1)	Mg2···H2	1.90(1)
N6–B1	1.438(2)	B1–N7	1.415(2)	N7–B2	1.523(2)
[**NN**-{MgNH(*i*Pr)BH$_3$}$_2$]·THF					
Mg1–N1	2.064(1)	Mg1–N5	2.087(1)	Mg1···H1	2.07(2)
Mg1–N2	2.078(1)	Mg1···B1	2.532(2)	Mg1···H2	2.11(2)
Mg1···H3	2.05(2)	B1–N5	1.581(2)	B2–N6	1.599(3)
Mg2–N3	2.028(1)	Mg2–N6	2.099(2)	Mg1···Mg2	3.7817(7)
Mg2–N4	2.061(1)	Mg2–O	2.034(1)		
[**NN**-Mg$_2$(*i*PrN-BH-*i*PrN-BH$_3$)]·THF					
Mg1–N1	2.047(1)	Mg1–N5	2.138(1)	Mg1···H1	2.06(2)
Mg1–N2	2.033(1)	Mg1···B1	2.324(1)	Mg1···H2	2.00(2)
Mg2–N3	2.042(1)	Mg2–N5	2.084(1)	N5–B1	1.456(2)
Mg2–N4	2.076(1)	Mg2–O	2.025(1)	B1–N6	1.414(2)
N6–B2	1.550(2)				

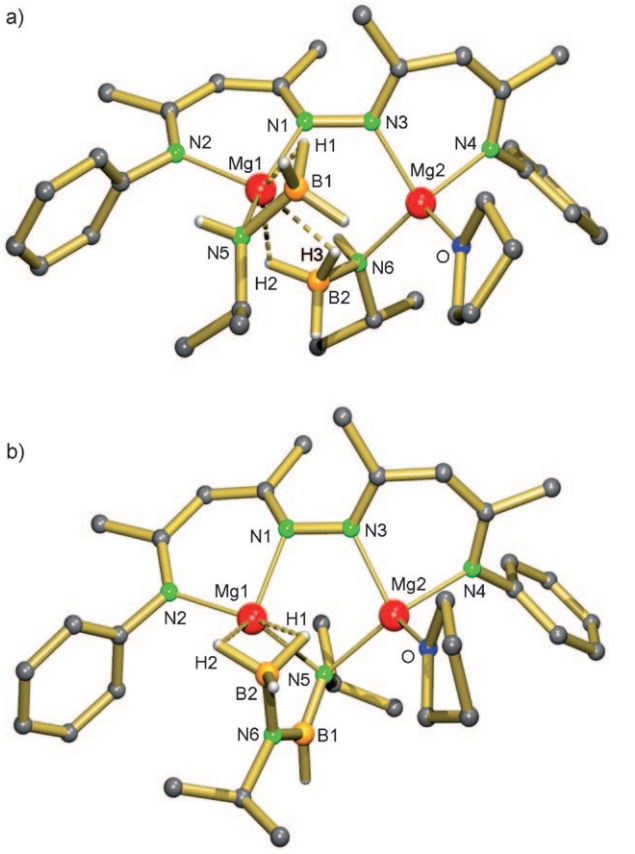

Figure 4. The crystal structures of a) [**NN**-{MgNH(*i*Pr)BH$_3$}$_2$]·THF and b) [**NN**-Mg$_2$(*i*PrN-BH-*i*PrN-BH$_3$)]·THF. For clarity, the *i*Pr substituents on the DIPPnacnac ligands have been omitted and only the hydrogen atoms on B and N are shown. Selected bond lengths are summarised in Table 2.

(*i*Pr)BH$_3$}$_2$] and [**NN**-{MgNH(*i*Pr)BH$_3$}$_2$] (Scheme 6). The crystal structure of [**PYR**-{MgNH(*i*Pr)BH$_3$}$_2$] is shown in Figure 3b. The asymmetric unit contains two nearly identical complexes, which, although roughly C_2-symmetric, show no exact crystallographic symmetry. The bond lengths given in Table 2 are average values for the four chemically different N atoms (N_a–N_d). The amidoborane anions bridge both Mg^{2+} ions in a similar fashion as observed for dimeric [{(DIPPnacnac)MgNH(*i*Pr)BH$_3$}$_2$]. Average Mg–N (2.123(4) Å) and Mg···B (2.449(5) Å) contacts compare well to those in [{(DIPPnacnac)MgN(*i*Pr)HBH$_3$}$_2$], 2.122(1) and 2.417(2) Å, respectively. Although [**NN**-{MgNH(*i*Pr)BH$_3$}$_2$] did not crystallise satisfactorily, addition of small amounts of THF gave good quality single crystals of the THF adduct [**NN**-{MgNH(*i*Pr)BH$_3$}$_2$]·THF (Figure 4a). The incorporation of only one THF ligand causes considerable asymmetry. One of the amidoborane units is side-on coordinated to Mg1, whereas the other bridges both Mg^{2+} ions in its usual fashion. The Mg–N and Mg···B contacts for bridging and side-on coordinated amidoborane anions are comparable to those in mononuclear Mg complexes. The Mg···Mg' contact length in the NN-coupled amidoborane complex (3.7817(7) Å) is somewhat longer than that in the pyridyl bridged complex (3.458(2) Å). At first sight it might be unexpected to observe the longer Mg···Mg' contact length in a complex without a bridging unit, however, it should be considered that the alignment of nacnac units in these ligand systems is different. It is expected that dynamic rotation around the N–N bond could give rise to a considerably smaller Mg···Mg' contact length.

Both binuclear Mg amidoborane complexes are easily soluble in benzene and were slowly heated while monitoring their decomposition by ^{1}H NMR spectroscopy. Whereas [**PYR**-{MgNH(*i*Pr)BH$_3$}$_2$] eliminates H_2 gas at 90 °C, [**NN**-{MgNH(*i*Pr)BH$_3$}$_2$] already decomposed at 60 °C. Therefore, binuclear Mg amidoborane complexes decompose at significantly lower temperatures than the comparable mononuclear species [(DIPPnacnac)MgNH(*i*Pr)BH$_3$]. The imposed spatial confinement of the two metal centres apparently has a significant effect on amidoborane decomposition. Not only is the decomposition temperature lowered by close proximity, but also the decomposition products are different.

In both cases, the decomposition reactions are clean and only a single species could be identified in the ^{1}H NMR spectra. The decomposition products could be crystallised and structurally characterisation by X-ray diffraction revealed BNBN species. The crystal structure of [**PYR**-

Mg_2(*i*PrN-BH-*i*PrN-BH_3)] is shown in Figure 3c. It features a dianionic BNBN unit that displays the typical bonding pattern we earlier observed in the decomposition products of Ca amidoborane complexes; the BN bonds in the *i*PrN-BH-N*i*Pr part are much shorter than the terminal *i*PrN-BH_3 bond. The dianionic species can be considered as a complex of the bora-amidinate[19] ligand *i*PrN-BH-N*i*Pr^{2-} and BH_3. The product of thermal decomposition of [**NN**-{MgNH(*i*Pr)-BH_3}$_2$] could only be crystallised after addition of small quantities of THF. The structure of the mono THF adduct is shown in Figure 4b. Coordination of THF to one of the Mg^{2+} ions causes asymmetrical bridging of the (*i*PrN-BH-*i*PrN-BH_3)$^{2-}$ ion. Whereas the Mg–N5 bond lengths are nearly equally long the BH_3 group only coordinates to one of the Mg^{2+} ions.

It is apparent that the here presented bimetallic Mg amidoborane complexes follow a decomposition pathway that is different from those for the corresponding monometallic Mg amidoboranes. Their enforced bimetallic nature should facilitate the BNBN-pathway outlined in Scheme 5. It is therefore likely that [(DIPPnacnac)MgNH(*i*Pr)BH_3], which is dimeric in the solid state, is at its rather high decomposition temperature of 110°C, not present as an aggregate.

Conclusion

Monometallic Mg amidoborane complexes with different substituents at the amidoborane N atom are easily accessible by deprotonation of the corresponding ammonia-borane with either a Mg amide or hydride base. In general, they decompose at higher temperatures than the analogue Ca amidoborane complexes and, in some cases, also different decomposition products are observed. Bimetallic Mg amidoborane complexes decompose at lower temperatures and give different products. From our studies we would like to draw the following conclusions:

i) *The first key step in the decomposition* of metal amidoborane complexes is the β-hydride elimination. This results in formation of a metal hydride intermediate and an aminoborane R(H)N=BH_2. The course of the follow-up reactions is dependent on the metal and the substituent R.

ii) *Metals* that are normally known to form mildly reactive reagents (like Zn^{2+}) would generate a rather stable metal hydride complex, which does not react further and can be isolated in high yield. In case of Ca^{2+}, however, the highly reactive hydride intermediate reacts immediately with the released R(H)N=BH_2. Compounds of Mg are intermediate in reactivity and in some cases the Mg hydride complex can be isolated, whereas in other cases further reaction takes place.

iii) *The fate of the intermediate aminoborane R(H)N=BH_2* strongly depends on the substituent R and the metal. Species with small substituents are highly reactive and either escape the metal's coordination sphere and oligomerise into [R(H)NBH_2]$_n$ or, depending on the reactivity of the metal intermediate, are attacked by the nucleophile [R(H)NBH_2]$^-$ to finally form the BNBN species (RN-BH-RN-BH_3)$^{2-}$. This is the low-energy pathway, which, depending on the metal, generally takes place at relatively low temperatures. An aminoborane with a large DIPP-substituent will not oligomerise, but can be deprotonated by the intermediate metal hydride to give the borylamide (DIPP)NBH_2^-. This is the high-energy pathway that needs more forcing conditions.

iv) *The nuclearity of the metal amidoborane complex* can influence the course of the decomposition pathway drastically. Enforced proximity of two Mg amidoborane units results in decomposition at a significantly lower temperature and cleanly follows the BNBN pathway, namely, the low-energy pathway. As the bimetallic amidoborane complexes presented here are a better model system for a multimetallic solid-state situation, the BNBN route should be considered a likely pathway for thermal decomposition of solid metal amidoborane salts like [M(NH_2BH_3)]$_\infty$ and [M(NH_2BH_3)$_2$]$_\infty$. A recent study on thermal hydrogen release in a series of alkali metal amidoboranes presents evidence that the BNBN route indeed is followed under solid state conditions.[20]

The mono- und dinuclear model systems presented here give valuable insight in the thermal release of hydrogen from metal amidoboranes. These solution studies could contribute to the rational design of a new class of solid-state hydrogen storage materials.

Experimental Section

All experiments were carried out under argon using standard Schlenk-techniques and freshly dried solvents. The following starting materials have been prepared according to literature: [(DIPPnacnac)MgN(SiMe_3)$_2$],[21] NH_3BH_3,[4a] $MeNH_2BH_3$,[4a] $DIPPNH_2BH_3$,[6] *i*PrNH_2BH_3[6] and [(DIPPnacnac)MgNH(DIPP)BH_3].[8] Di-*n*-butylmagnesium solution in heptane was purchased from ACROS and used as received.

[(DIPPnacnac)MgNH_2BH_3]: A solution of NH_3BH_3 (18 mg, 0.583 mmol) in THF (0.1 mL) was added to a solution of [(DIPP-nacnac)MgN(SiMe_3)$_2$] (240 mg, 0.398 mmol) in benzene (3.0 mL). When the reaction mixture was left to stand overnight at room temperature, colourless crystals of [(DIPPnacnac)MgNH_2BH_3] formed. Yield: 160 mg, 0.339 mmol, 85%. Recrystallisation from a hexane/THF mixture gave crystals of the THF adduct [(DIPPnacnac)MgNH_2BH_3]·THF suitable for single-crystal X-ray diffraction. ^{1}H{^{11}B} NMR (300 MHz, [D_6]benzene/[D_8]THF 4/1, 20°C, TMS): $\delta = -0.51$ (q, ^3J(H,H) = 6.0 Hz, 2H; NH_2), 1.19 (d, ^3J(H,H) = 6.9 Hz, 12H; *i*Pr), 1.22 (d, ^3J(H,H) = 6.9 Hz, 12H; *i*Pr), 1.62 (s, 6H; Me backbone), 1.77 (t (br), 3H; BH_3), 3.20 (sept, ^3J(H,H) = 6.9 Hz, 4H; *i*Pr), 4.78 (s, 1H; H backbone), 7.10–7.13 (m, 5H; aryl), 7.21 ppm (m, 1H; aryl); ^{11}B NMR (160 MHz, [D_6]benzene/[D_8]THF 4/1, 20°C, BF_3·OEt_2): $\delta = -22.4$ ppm (q, ^1J(B,H) = 87.2 Hz); ^{13}C NMR (75 MHz, [D_6]benzene/[D_8]THF 4/1, 20°C, TMS): δ = 24.5 (*i*Pr), 24.6 (*i*Pr), 25.0 (Me backbone), 28.2 (*i*Pr), 94.8 (backbone), 124.8 (aryl), 125.1 (aryl), 142.4 (aryl), 146.5 (aryl), 168.5 ppm (backbone); elemental analysis (%) calcd for $C_{29}H_{46}BMgN_3$ (M_r = 471.83): C 73.82, H 9.83; found: C 73.56, H 9.85.

[(DIPPnacnac)MgNH(Me)BH_3]·THF: A solution of $MeNH_2BH_3$ (15 mg, 0.334 mmol) in THF (0.1 mL) was added to a solution of

[(DIPPnacnac)MgN(SiMe$_3$)$_2$] (200 mg, 0.332 mmol) in benzene (2.0 mL). When the reaction mixture was left to stand overnight at room temperature, colourless crystals of [(DIPPnacnac)MgNH(Me)BH$_3$]·THF formed. Yield: 138 mg, 0.247 mmol, 74%. ^{1}H{^{11}B} NMR (500 MHz, [D$_6$]benzene/[D$_8$]THF 4/1, 20°C, TMS): $\delta = -0.40$ (m, 1H; NH), 1.15 (d, ^3J(H,H) = 6.9 Hz, 12H; *i*Pr), 1.23 (d, ^3J(H,H) = 6.9 Hz, 12H; *i*Pr), 1.47 (m, 4H; THF), 1.60 (s, 6H; Me backbone), 1.63 (d, ^3J(H,H) = 4.6 Hz, 3H; BH$_3$), 1.64 (d, ^3J(H,H) = 6.5 Hz, 3H; NMe), 3.18 (sept, ^3J(H,H) = 6.9 Hz, 4H; *i*Pr), 3.53 (m, 4H; THF), 4.77 (s, 1H; H backbone), 7.07–7.08 ppm (m, 6H; aryl); ^{11}B NMR (160 MHz, [D$_6$]benzene/[D$_8$]THF 4/1, 20°C, BF$_3$·OEt$_2$): $\delta = -19.0$ ppm (q, ^1J(B,H) = 86.5 Hz); ^{13}C NMR (75 MHz, [D$_6$]benzene/[D$_8$]THF 4/1, 20°C, TMS): $\delta = 24.5$ (*i*Pr), 24.7 (*i*Pr), 24.8 (Me backbone), 25.8 (THF), 28.2 (*i*Pr), 37.2 (NMe), 67.8 (THF), 94.9 (backbone), 123.8 (aryl), 125.1 (aryl), 142.4 (aryl), 146.8 (aryl), 168.5 ppm (backbone); elemental analysis (%) calcd for C$_{34}$H$_{56}$BMgN$_3$O (M_r = 557.94): C 73.19, H 10.12; found: C 72.88, H 9.72.

[(DIPPnacnac)MgNH(*i*Pr)BH$_3$]: *i*PrNH$_2$BH$_3$ (24 mg, 0.329 mmol) and [(DIPPnacnac)MgN(SiMe$_3$)$_2$] (200 mg, 0.332 mmol) were dissolved in benzene (2.0 mL) and the reaction mixture was allowed to stand overnight. This resulted in the precipitation of colourless crystals of the product [(DIPPnacnac)MgNH(*i*Pr)BH$_3$]. Yield: 153 mg, 0.298 mmol, 90%. ^{1}H{^{11}B} NMR (500 MHz, [D$_6$]benzene/[D$_8$]THF 4/1, 20°C, TMS): $\delta = -0.41$ (m, 1H; NH), 0.69 (d, ^3J(H,H) = 5.2 Hz, 6H; N*i*Pr), 1.20 (d, ^3J(H,H) = 6.9 Hz, 12H; *i*Pr), 1.30 (d, ^3J(H,H) = 6.9 Hz, 12H; *i*Pr), 1.59 (d, ^3J(H,H) = 5.1 Hz, 3H; BH$_3$), 1.64 (s, 6H; Me backbone), 2.39 (m, 1H; N*i*Pr), 3.22 (sept, ^3J(H,H) = 6.9 Hz, 4H; *i*Pr), 4.82 (s, 1H; H backbone), 7.11–7.14 ppm (m, 6H; aryl); ^{11}B NMR (160 MHz, [D$_6$]benzene/[D$_8$]THF 4/1, 20°C, BF$_3$·OEt$_2$): $\delta = -22.0$ ppm (q, ^1J(B,H) = 88.4 Hz); ^{13}C NMR (75 MHz, [D$_6$]benzene/[D$_8$]THF 4/1, 20°C, TMS): $\delta = 24.2$ (N*i*Pr), 24.6 (*i*Pr), 24.8 (*i*Pr), 24.9 (Me backbone), 28.4 (*i*Pr), 48.8 (N*i*Pr), 95.0 (backbone), 123.9 (aryl), 125.2 (aryl), 142.4 (aryl), 147.3 (aryl), 168.4 ppm (backbone); elemental analysis (%) calcd for C$_{32}$H$_{52}$BMgN$_3$ (M_r = 513.89): C 74.79, H 10.20; found: C 74.61, H 10.51.

[PYR-{Mg(*n*Bu)}$_2$]: To a solution of Mg(*n*Bu)$_2$ in heptane (0.5 M in heptane, 5.08 mL, 2.540 mmol) and benzene (5 mL) was added **PYR**-H$_2$ (750 mg, 1.267 mmol). After the evolution of gas ceased, the dark red solution was stirred for one additional hour. All volatile compounds were removed under vacuum and the crude product was dissolved in hot hexane (5 mL). Cooling the solution slowly to 5°C gave yellow crystals suitable for X-ray analysis. Yield: 414 mg, 0.550 mmol, 43%. ^{1}H NMR (300 MHz, [D$_6$]benzene, TMS): $\delta = -0.44$ (m, 4H; *n*Bu), 0.92 (t, ^3J(H,H) = 6.8 Hz, 6H; *n*Bu), 1.07 (d, ^3J(H,H) = 6.8 Hz, 12H; *i*Pr), 1.16 (d, ^3J(H,H) = 6.8 Hz, 12H; *i*Pr), 1.32–1.40 (m, 8H; *n*Bu), 1.65 (s, 6H; Me backbone), 2.08 (s, 6H; *i*Pr), 3.16 (sept, ^3J(H,H) = 6.8 Hz 4H; *i*Pr), 4.83 (s, 2H; backbone), 6.25 (d, ^3J(H,H) = 8.0 Hz, 2H; aryl), 7.06–7.13 ppm (m, 7H; aryl); ^{13}C NMR (75 MHz, [D$_6$]benzene, TMS): $\delta = 6.93$ (*n*Bu), 15.2 (*n*Bu), 24.6 (*i*Pr), 24.8 (*i*Pr), 25.5 (*i*Pr), 25.8 (*i*Pr), 28.9 (*i*Pr), 31.3 (*n*Bu), 31.6 (*n*Bu), 100.7 (backbone), 107.2 (aryl), 124.7 (aryl), 126.2 (aryl), 140.9 (aryl), 142.2 (aryl), 160.4 (aryl), 162.4 (aryl), 172.5 (backbone), 171.7 ppm (backbone); elemental analysis (%) calcd for C$_{47}$H$_{69}$Mg$_2$N$_5$ (M_r = 752.69): C 75.00, H 9.24; found: C 74.78, H 9.10.

PYR-[MgNH(*i*Pr)BH$_3$]$_2$: A solution of [**PYR**-{Mg(*n*Bu)}$_2$] (180 mg, 0.239 mmol) and *i*PrNH$_2$BH$_3$ (35 mg, 0.479 mmol) in benzene (4.0 mL) was stirred for two hours at room temperature. The solution was concentrated to a volume of approximately 1 mL and slowly cooled to 8°C. The desired product precipitated from this solution in the form of yellow crystalline blocks. Yield: 169 mg, 0.216 mmol, 90%. ^{1}H{^{11}B} NMR (500 MHz, [D$_6$]benzene, 20°C, TMS): $\delta = 0.51$, (br, 2H; NH*i*Pr), 1.04 (d, ^3J(H,H) = 6.9 Hz, 6H; *i*Pr), 1.09 (d, ^3J(H,H) = 6.9 Hz, 6H; *i*Pr), 1.11 (d, ^3J(H,H) = 6.4 Hz, 6H; NH*i*Pr), 1.12 (d, ^3J(H,H) = 6.4 Hz, 6H; NH*i*Pr), 1.28 (d, ^3J(H,H) = 6.9 Hz, 6H; *i*Pr), 1.41 (d, ^3J(H,H) = 6.9 Hz, 6H; *i*Pr), 1.46 (br, 6H; BH$_3$), 1.59 (s, 6H; Me backbone), 2.13 (s, 6H; Me backbone), 3.12 (sept, ^3J(H,H) = 6.9 Hz, 2H; *i*Pr), 3.17 (sept, ^3J(H,H) = 6.9 Hz, 2H; *i*Pr), 3.28 (sept, ^3J(H,H) = 6.9 Hz, 2H; NH*i*Pr), 4.88 (s, 2H; H backbone), 6.20 (d, ^3J(H,H) = 8.1 Hz, 2H; aryl), 6.99 (t, ^3J(H,H) = 8.1 Hz, 1H; aryl), 7.02 (dd, ^3J(H,H) = 7.5 Hz, ^4J(H,H) = 1.6 Hz, 2H; aryl), 7.14 ppm (dd, ^3J(H,H) = 7.5 Hz, ^4J(H,H) = 1.6 Hz, 2H; aryl); ^{11}B NMR (160 MHz, [D$_6$]benzene, 20°C, BF$_3$·OEt$_2$): $\delta = -23.6$ ppm (q, br); ^{13}C NMR (75 MHz, [D$_6$]benzene, 20°C, TMS): $\delta = 22.7$ (Me backbone), 23.0 (Me backbone), 24.6 (*i*Pr), 24.9 (NH*i*Pr), 25.0 (NH*i*Pr), 25.2 (*i*Pr), 25.3 (*i*Pr), 25.4 (*i*Pr), 28.6 (*i*Pr), 28.9 (*i*Pr), 49.1 (NH*i*Pr), 102.4 (backbone), 107.7 (aryl), 124.1 (aryl), 125.0 (aryl), 126.3 (aryl), 139,4 (aryl), 140.8 (aryl), 142.3 (aryl), 145.3 (aryl), 161.4 (backbone), 161.9 (backbone), 172.2 ppm (aryl); elemental analysis (%) calcd for C$_{45}$H$_{73}$B$_2$Mg$_2$N$_7$ (M_r = 782.34): C 69.09, H 9.41; found: C 68.63, H 9.80.

[NN-{Mg(*n*Bu)}$_2$]: To a solution of Mg(*n*Bu)$_2$ in heptane (1.0 M in heptane, 3.90 mL, 3.90 mmol) was added **NN**-H$_2$ (1.00 g, 1.94 mmol) in portions. After one hour a yellow solid precipitated from the orange solution. The solid was isolated by centrifugation and subsequent removal of the mother liquor. After washing with pentane and drying under vacuum (0.01 Torr, 10 min) a microcrystalline product was obtained. Yield: 810 mg, 1.199 mmol, 62%. ^{1}H NMR (300 MHz, [D$_6$]benzene + trace [D$_8$]THF): $\delta = -0.52$ (b, 4H; *n*Bu), 0.88 (t, ^3J(H,H) = 7.2 Hz, 6H; *n*Bu), 1.17–1.40 (m, 32H; *i*Pr and *n*Bu), 1.67 (s, 6H; Me backbone), 2.05 (s, 6H; Me backbone), 3.13 (m, 2H; *i*Pr), 3.29 (m, 2H; *i*Pr), 4.63 (s, 2H; backbone), 7.12–7.16 ppm (m, 6H; aryl). ^{13}C NMR (75 MHz, [D$_8$]THF): $\delta = 7.3$ (*n*Bu), 14.7 (*n*Bu), 22.8 (Me backbone), 24.5 (Me backbone), 25.0 (*i*Pr), 25.2 (*i*Pr), 25.6 (*i*Pr), 28.8 (*i*Pr), 29.1 (*i*Pr), 33.0 (*n*Bu), 33.5 (*n*Bu), 92.2 (HC backbone), 124.1 (aryl), 124.6 (aryl), 125.5 (aryl), 143.3 (aryl), 143.9 (aryl), 147.5 (aryl), 166.5 (MeC backbone), 166.9 ppm (MeC backbone).

[NN-{MgNH(*i*Pr)BH$_3$}$_2$]: A solution of [**NN**-{Mg(*n*Bu)}$_2$] (460 mg, 0.681 mmol) and *i*PrNH$_2$BH$_3$ (100 mg, 1.371 mmol) in benzene (12.0 mL) was stirred for one hour at room temperature. The solution was concentrated to about 4 mL and slowly cooled to 8°C. The desired product precipitated in form of yellow blocks. Yield: 313 mg, 0.444 mmol, 65%. ^{1}H-{^{11}B} NMR (500 MHz, [D$_8$]THF, 20°C, TMS): $\delta = -0.17$, (br, 2H; NH*i*Pr), 0.49 (d, ^3J(H,H) = 6.3 Hz, 6H; NH*i*Pr), 0.73 (d, ^3J(H,H) = 6.3 Hz, 6H; NH*i*Pr), 1.07 (d, ^3J(H,H) = 6.8 Hz, 6H; *i*Pr), 1.18 (d, ^3J(H,H) = 6.8 Hz, 6H; *i*Pr), 1.20 (d, ^3J(H,H) = 6.8 Hz, 6H; *i*Pr), 1.23 (d, ^3J(H,H) = 6.8 Hz, 6H; *i*Pr), 1.67 (s, 6H; Me backbone), 1.89 (br, 6H; BH$_3$), 1.93 (s, 6H; Me backbone), 2.34 (sept, ^3J(H,H) = 6.3 Hz, 1H; NH*i*Pr), 2.37 (sept, ^3J(H,H) = 6.3 Hz, 1H; NH*i*Pr), 3.22 (sept, ^3J(H,H) = 6.8 Hz, 2H; *i*Pr), 3.25 (sept, ^3J(H,H) = 6.8 Hz, 2H; *i*Pr), 4.57 (s, 2H; H backbone), 7.00–7.12 ppm (m, 6H; aryl); ^{11}B NMR (160 MHz, [D$_8$]THF, 20°C, BF$_3$·OEt$_2$): $\delta = -21.6$ ppm (q, br, BH$_3$); ^{13}C NMR (75 MHz, [D$_8$]THF, 20°C, TMS): $\delta = 22.3$ (Me backbone), 24.33 (NH*i*Pr), 25.02 (Me backbone), 25.2 (*i*Pr), 25.7 (*i*Pr), 25.8 (*i*Pr), 25.9 (*i*Pr), 26.5 (NH*i*Pr), 28.8 (*i*Pr), 28.9 (*i*Pr), 50.5 (NH*i*Pr), 92.3 (backbone), 124.9 (aryl), 124.9 (aryl), 125.8 (aryl), 143.9 (aryl), 144.2 (aryl), 148.1 (aryl), 167.2 ppm (backbone); elemental analysis (%) calcd for C$_{40}$H$_{70}$B$_2$Mg$_2$N$_6$ (M_r = 705.26): C 68.12, H 10.00; found: C 67.68, H 10.10. Crystals suitable for X-ray analysis were obtained by addition of small amounts of THF to a concentrated solution of [**NN**-{MgNH(*i*Pr)-BH$_3$}$_2$] in benzene and subsequent cooling to 8°C. This resulted in the crystallisation of the THF-adduct [**NN**-{MgNH(*i*Pr)BH$_3$}$_2$]·THF.

General procedure for the thermal decomposition of Mg amidoborane complexes: The corresponding amidoborane (30–40 mg) was dissolved in deuterated benzene (0.5 mL) and filled in a J. Young NMR-tube. The sample was heated gradually and the progress of the decomposition was monitored by measuring ^{1}H NMR spectra in regular intervals. For synthetic purposes larger tubes with teflon fittings can be used.

Decomposition of [(DIPPnacnac)MgNH(*i*Pr)BH$_3$] and isolation of [(DIPPnacnac)MgH]: [(DIPPnacnac)MgNH(*i*Pr)BH$_3$] (75 mg, 0.147 mmol) was dissolved in benzene (2.7 mL) and heated for 16 h at 110°C. Then the solvent was evaporated in vacuo and the residue was triturated with hexane (0.8 mL). The remaining white powder of [(DIPPnacnac)MgH] was separated, washed with hexane and dried in vacuo. Yield 58 mg, 0.131 mmol, 89%. ^{1}H and ^{13}C NMR spectra compare with those published earlier.[11] Crystals of the THF adduct [{(DIPPnacnac)MgH·THF}$_2$] suitable for X-ray analysis were formed upon recrystallisation of the white powder from a hexane/THF mixture. From NMR spectra we conclude that the amidoborane part cleanly reacted to the borazine (*i*PrNBH)$_3$: ^{1}H{^{11}B} NMR (500 MHz, [D$_6$]benzene, 20°C, TMS): $\delta = 1.25$ (d, ^3J(H,H) = 6.7 Hz, 18H; N*i*Pr), 3.67 (sept, ^3J(H,H) = 6.7 Hz, 3H; N*i*Pr), 4.95 ppm (br, 3H; BH), ^{13}C{^{1}H}, $\delta = 26.6$ (*i*Pr), 52.1 ppm

(*i*Pr); $^{11}B\{^1H\}$ NMR (500 MHz, [D$_6$]benzene, 20 °C, TMS): $\delta = 32.5$ ppm (d, $^1J(B,H) = 132$ Hz, BH). These measurements are in agreement with literature data for (*i*PrN-BH)$_3$.[22]

Decomposition of [(DIPPnacnac)MgNH(DIPP)BH$_3$] and isolation of [(DIPPnacnac)MgN(DIPP)BH$_2$]: A solution of [(DIPPnacnac)MgNH-(DIPP)BH$_3$] (120 mg, 0.189 mmol) in benzene (8.0 mL) was heated in a closed tube (with teflon seal) for 24 h at 120 °C. After evaporation of the solvent in vacuo a sticky solid remained which was dissolved in hexane (1.2 mL), toluene (0.6 mL), and THF (0.6 mL). Subsequent cooling of this solution to −27 °C gave colourless crystals of [(DIPPnacnac)MgN-(DIPP)BH$_2$]·THF. Yield: 37 mg, 0.053 mmol, 28 %. $^1H\{^{11}B\}$ NMR (500 MHz, [D$_6$]benzene/[D$_8$]THF, 20 °C, TMS): $\delta = 0.51$ (br, 6H; *i*Pr amidoborane), 0.89 (d, $^3J(H,H) = 6.5$ Hz, 6H; *i*Pr amidoborane), 1.17 (d, ^3J-(H,H) = 5.9 Hz, 12H; *i*Pr nacnac), 1.26 (br, 12H; *i*Pr nacnac), 1.73 (m (br), 4H; THF), 1.77 (s, 6H; Me backbone), 2.28 (br, 2H; *i*Pr amidoborane), 3.30 (br, 4H; *i*Pr), 3.58 (m (br), 4H; THF), 4.29 (br, 1H; BH$_2$), 4.76 (br, 1H; BH$_2$), 4.91 (s, 1H; H backbone), 6.60 (t, $^3J(H,H) = 7.6$ Hz, 1H; aryl), 6.75 (d, $^3J(H,H) = 7.6$ Hz, 2H; aryl), 7.15–7.18 ppm (m, 6H; aryl); ^{11}B NMR (160 MHz, [D$_6$]benzene/[D$_8$]THF, 20 °C, $BF_3{\cdot}OEt_2$): $\delta =$ 33.9 ppm (br); ^{13}C NMR (75 MHz, [D$_6$]benzene, 20 °C): $\delta = 14.3$ (*i*Pr amidoborane), 23.1 (*i*Pr amidoborane), 24.3 (*i*Pr), 25.3 (br, *i*Pr), 25.9 (THF), 26.2 (Me backbone), 27.9 (*i*Pr), 28.4 (br, *i*Pr), 32.0 (*i*Pr amidoborane), 67.8 (THF), 93.9 (backbone), 121.0 (aryl amidoborane), 122.4 (aryl), 124.2 (aryl amidoborane), 125.5 (aryl), 140.0 (aryl), 142.8 (aryl amidoborane), 146.0 (aryl), 154.5 (aryl amidoborane), 168.8 ppm (backbone); elemental analysis (%) calcd for $C_{45}H_{68}BMgN_3O$ ($M_r = 702.16$): C 76.97, H 9.76; found: C 77.29, H 9.81.

Decomposition of [PYR-{MgNH(*i*Pr)BH$_3$}$_2$] and isolation of [PYR-Mg$_2$(*i*PrN-BH-*i*PrN-BH$_3$)]: A solution of [**PYR**-{MgNH(*i*Pr)BH$_3$}$_2$] (220 mg, 0.281 mmol) in benzene (4.0 mL) was heated to 90 °C for three days. Then the solvent was evaporated and hexane (0.8 mL) was added. Upon standing overnight at room temperature, [**PYR**-Mg$_2$(*i*PrN-BH-*i*PrN-BH$_3$)] precipitated as a yellow powder. Crystals suitable for X-ray analysis were obtained by slowly cooling a concentrated hexane solution to −27 °C. Yield: 113 mg, 0.145 mmol, 52 %. $^1H\{^{11}B\}$ NMR (500 MHz, [D$_6$]benzene, 20 °C, TMS): $\delta = 0.31$ (d, $^3J(H,H) = 6.5$ Hz, 6H; NH*i*Pr), 1.02 (d, $^3J(H,H) = 6.7$ Hz, 6H; NH*i*Pr), 1.17 (d, $^3J(H,H) = 6.8$ Hz, 6H; *i*Pr), 1.37 (d, $^3J(H,H) = 6.8$ Hz, 6H; *i*Pr), 1.41 (d, $^3J(H,H) = 6.2$ Hz, 6H; *i*Pr), 1.48 (d, $^3J(H,H) = 6.7$ Hz, 6H; *i*Pr), 1.56 (s, 6H; Me backbone), 1.97 (s, 6H; Me backbone), 2.00 (br, 3H; BH$_3$), 3.13 (sept, $^3J(H,H) = 6.5$ Hz, 1H; NH*i*Pr), 3.14 (sept, $^3J(H,H) = 6.7$ Hz, 2H; *i*Pr), 3.23 (sept, $^3J(H,H) =$ 6.8 Hz, 2H; *i*Pr), 3.72 (sept, $^3J(H,H) = 6.2$ Hz, 1H; NH*i*Pr), 4.86 (s, 2H; H backbone), 4.93 (br, 1H; BH), 6.10 (d, $^3J(H,H) = 8.0$ Hz, 2H; aryl), 6.98 (t, $^3J(H,H) = 8.0$ Hz, 1H; aryl) 7.05–7.10 ppm (m, 6H; aryl); ^{11}B NMR (160 MHz, [D$_6$]benzene, 20 °C, $BF_3{\cdot}OEt_2$): $\delta = -20.91$ (q (br), BH$_3$), 36.00 ppm (br, BH); ^{13}C NMR (75 MHz, [D$_6$]benzene, 20 °C, TMS): $\delta = 23.8$ (Me backbone), 25.0 (*i*Pr), 25.0 (N*i*Pr), 25.0 (*i*Pr), 25.3 (*i*Pr), 25.4 (*i*Pr), 26.1 (Me backbone), 28.9 (*i*Pr), 29.3 (*i*Pr), 29.6 (N*i*Pr), 50.9 (N*i*Pr), 53.4 (N*i*Pr), 100.5 (backbone), 108.5 (aryl), 124.5 (aryl), 125.4 (aryl), 126.5 (aryl), 140,4 (aryl), 141.6 (aryl), 142.7 (aryl), 147.3 (aryl), 161.4 (backbone), 162.1 (backbone), 173.5 ppm (aryl); elemental analysis (%) calcd for $C_{45}H_{69}B_2Mg_2N_7$ ($M_r = 778.31$): C 69.44, H 8.94; found: C 68.78, H 8.99.

Decomposition of [NN-{MgNH(*i*Pr)BH$_3$}$_2$] and isolation of [NN-Mg$_2$(*i*PrN-BH-*i*PrN-BH$_3$)]: A solution of [**NN**-{MgNH(*i*Pr)BH$_3$}$_2$] (100 mg, 0.142 mmol) in benzene (3.0 mL) was heated to 60 °C for 18 h. The solvent was evaporated and hexane (0.6 mL) was added. Cooling this solution to −27 °C resulted in precipitation of [**NN**-Mg$_2$(*i*PrN-BH-*i*PrN-BH$_3$)] as a yellow powder. Yield: 44 mg, 0.063 mmol, 44 %. $^1H\{^{11}B\}$ NMR (500 MHz, [D$_6$]benzene, 20 °C, TMS): $\delta = 0.70$ (d, $^3J(H,H) =$ 6.5 Hz, 3H; NH*i*Pr), 0.84 (d, $^3J(H,H) = 6.5$ Hz, 3H; NH*i*Pr), 0.96 (d, ^3J-(H,H) = 6.5 Hz, 3H; NH*i*Pr), 1.12 (d, $^3J(H,H) = 6.8$ Hz, 3H; *i*Pr), 1.17–1.21 (m, 15H; *i*Pr and NH*i*Pr), 1.28 (d, $^3J(H,H) = 6.8$ Hz, 3H; *i*Pr), 1.32 (d, $^3J(H,H) = 6.8$ Hz, 3H; *i*Pr), 1.34 (d, $^3J(H,H) = 6.8$ Hz, 3H; *i*Pr), 1.67 (s, 3H; Me backbone), 1.70 (s, 3H; Me backbone), 1.83 (s, 6H; Me backbone), 2.13 (br, 3H; BH$_3$), 3.13 (sept, $^3J(H,H) = 6.8$ Hz, 1H; *i*Pr), 3.25 (sept, $^3J(H,H) = 6.5$ Hz, 1H; NH*i*Pr), 3.30 (sept, $^3J(H,H) = 6.8$ Hz, 1H; *i*Pr), 3.35 (sept, $^3J(H,H) = 6.8$ Hz, 1H; *i*Pr), 3.36 (sept, (H,H) = 6.8 Hz, 1H; *i*Pr), 3.42 (sept, $^3J(H,H) = 6.5$ Hz, 1H; NH*i*Pr), 4.61 (s, 1H; H backbone), 4.64 (s, 1H; H backbone), 5.12 (br, 1H; BH), 7.04–7.13 ppm (m, 6H; aryl); ^{11}B NMR (160 MHz, [D$_6$]benzene, 20 °C, $BF_3{\cdot}OEt_2$): $\delta =$ −21.12 (q, $^1J(B,H) = 79.5$ Hz, BH$_3$), 39.20 ppm (br, BH); ^{13}C NMR (75 MHz, [D$_6$]benzene, 20 °C, TMS): $\delta = 20.6$ (Me backbone), 21.0 (Me backbone), 23.5 (N*i*Pr), 23.9 (N*i*Pr), 24.1 (Me backbone), 24.1 (Me backbone), 24.4 (*i*Pr), 24.4 (*i*Pr), 25.1 (*i*Pr), 25.2 (*i*Pr), 25.4 (*i*Pr), 26.3 (*i*Pr), 28.5 (N*i*Pr), 28.7 (*i*Pr), 28.8 (*i*Pr), 29.0 (*i*Pr), 29.4 (*i*Pr), 31.5 (N*i*Pr), 50.5 (N*i*Pr), 53.4 (N*i*Pr), 91.5 (backbone), 92.6 (backbone), 124.4 (aryl), 124.7 (aryl), 124.7 (aryl), 124.7 (aryl), 126.0 (aryl), 126.1 (aryl), 142.8 (aryl), 143.0 (aryl), 143,4 (aryl), 143.7 (aryl), 145.1 (aryl), 145.9 (aryl), 166.4 (backbone), 167.0 (backbone), 167.8 (backbone) 169.4 ppm (backbone); elemental analysis (%) calcd for $C_{40}H_{66}B_2Mg_2N_6$ ($M_r = 701.22$): C 68.51, H 9.49; found: C 68.01, H 9.34. Crystals suitable for X-ray analysis could be obtained by slowly cooling a concentrated hexane/THF solution to −27 °C. In the presence of THF, crystals of [**NN**-Mg$_2$(*i*PrN-BH-*i*PrN-BH$_3$)]·THF were obtained.

Crystal structures: CCDC 760594–760603 contain the supplementary crystallographic data for this paper (for number assignment see Table S1 in the Supporting Information). These data can be obtained free of charge from The Cambridge Crystallographic Data Centre via www.ccdc.cam.ac.uk/data_request/cif.

Acknowledgements

We thank Prof. Dr. R. Boese and D. Bläser for collection of the X-ray data and acknowledge the DFG for financial support.

[1] Z. Xiong, C. K. Yong, G. Wu, P. Chen, W. Shaw, A. Karkamkar, T. Autrey, M. O. Jones, S. R. Johnson, P. P. Edwards, W. I. F. David, *Nat. Mater.* **2008**, *7*, 138–141.
[2] H. V. K. Diyablanage, R. P. Shrestha, T. A. Semelsberger, B. L. Scott, M. E. Bowden, B. L. Davis, A. K. Burrell, *Angew. Chem.* **2007**, *119*, 9153–9155; *Angew. Chem. Int. Ed.* **2007**, *46*, 8995–8997.
[3] For recent reviews, see: a) T. B. Marder, *Angew. Chem.* **2007**, *119*, 8262–8264; *Angew. Chem. Int. Ed.* **2007**, *46*, 8116–8118; b) F. H. Stephens, V. Pons, R. T. Baker, *Dalton Trans.* **2007**, 2613–2626; c) T. J. Clark, K. Lee, I. Manners, *Chem. Eur. J.* **2006**, *12*, 8634–8648; d) A. Karkambar, C. Aardahl, T. Autrey, *Mater. Matters* **2007**, *2*, 6–10; e) N. C. Smythe, J. C. Gordon, *Eur. J. Inorg. Chem.* **2010**, 509–521.
[4] a) P. V. Ramachandran, P. D. Gagare, *Inorg. Chem.* **2007**, *46*, 7810–7817; b) B. L. Davis, D. A. Dixon, E. B. Garner, J. C. Gordon, M. H. Matus, B. Scott, F. H. Stephens, *Angew. Chem.* **2009**, *121*, 6944–6948; *Angew. Chem. Int. Ed.* **2009**, *48*, 6812–6816.
[5] J. Spielmann, G. Jansen, H. Bandmann, S. Harder, *Angew. Chem.* **2008**, *120*, 6386–6391; *Angew. Chem. Int. Ed.* **2008**, *47*, 6290–6295.
[6] J. Spielmann, S. Harder, *J. Am. Chem. Soc.* **2009**, *131*, 5064–5065.
[7] J. Spielmann, D. Piesik, B. Wittkamp, G. Jansen, S. Harder, *Chem. Commun.* **2009**, 3455–3456.
[8] J. Spielmann, M. Bolte, S. Harder, *Chem. Commun.* **2009**, 6934–6936.
[9] D. Y. Kim, N. J. Singh, H. M. Lee, K. S. Kim, *Chem. Eur. J.* **2009**, *15*, 5598–5604.
[10] T. B. Lee, M. L. McKee, *Inorg. Chem.* **2009**, *48*, 7564–7575.
[11] S. P. Green, C. Jones, A. Stasch, *Angew. Chem.* **2008**, *120*, 9219–9223; *Angew. Chem. Int. Ed.* **2008**, *47*, 9079–9083.
[12] C. Ruspic, J. Spielmann, S. Harder, *Inorg. Chem.* **2007**, *46*, 5320–5326.
[13] R. D. Shannon, *Acta Crystallogr. Sect. A* **1976**, *32*, 751–767.
[14] M. H. Matus, K. D. Anderson, D. M. Camaioni, S. T. Autrey, D. A. Dixon, *J. Phys. Chem. A* **2007**, *111*, 4411–4421.
[15] W. T. Klooster, T. F. Koetzle, P. E. M. Siegbahn, T. B. Richardson, R. H. Crabtree, *J. Am. Chem. Soc.* **1999**, *121*, 6337–6343.

[16] E. Karwacki, G. Jansen, S. Harder, unpublished results.
[17] D. F.-J. Piesik, S. Range, S. Harder, *Organometallics* **2008**, *27*, 6178–6187.
[18] D. F.-J. Piesik, R. Stadler, S. Range, S. Harder, *Eur. J. Inorg. Chem.* **2009**, 3569–3576.
[19] See for a review, see: C. Fedorchuk, M. Copsey, T. Chivers, *Coord. Chem. Rev.* **2007**, *251*, 897–924.
[20] A. T. Luedtke, T. Autrey, *Inorg. Chem.* **2010**, 49, 3905–3910.
[21] D. J. Williams, A. J. P. White, J. A. Segal, E. L. Marshall, H. Pimpa, V. C. Gibson, A. P. Dove, *Dalton Trans.* **2003**, *15*, 3088–3097.
[22] E. Framery, M. Vaultier, *Heteroat. Chem.* **2000**, *11*, 218–225.

Received: January 6, 2010
Published online: June 16, 2010

